Journal of Material Chemistry C

ARTICLE

Supporting Information

Organic-Inorganic Hybrid Perovskite Logic Gate for Better Computing

Guoming Lin,[a,b] Yuanwei Lin,[c,d] Rongli Cui,[a] Huan Huang,[a] Xihong Guo,[a] Cheng Li,[a,b] Jinquan Dong,[a] Xuefeng Guo[c,e] and Baoyun Sun*[a]

Experimental

$CH_3NH_3PbI_3$ film synthesis and characterization: PbI_2 was purchased from Alfa Aesar without further purification. PbI_2 and CH_3NH_3I (MAI) were dissolved into dimethylformamide (DMF) and 2-propanol with concentrations of 450 mg ml^{-1} for PbI_2 and 55 mg ml^{-1} for MAI, respectively. PbI_2 was heated at 65 °C for about 30 min to make sure it was fully dissolved. The PbI_2 solution was spin-cast on the top of PEDOT:PSS covered ITO substrate at 5,000 r/min for 30 s. The MAI solution was spin-cast on the top of PbI_2 film at 5,000 r/min for 20 s at room temperature subsequently. The spin-cast PbI_2/MAI stacking films were thermally annealed at 100 °C for 2h. The X-ray diffraction pattern was collected on a Bruker D8-Advance x-ray powder diffractometer with Cu Kα radiation (λ = 1.5406 Å) and a step size of 0.02°. The scanning electron microscope image was taken on a Hitachi S4800 with an acceleration voltage of 5 kV. Tapping mode atomic force microscope image was performed on a Bruker Dimension EDGE. The electronic absorption spectroscopy was carried out in an Agilent Cary 5000 UV-Visible spectrometer.

Device Fabrication and characterization: After the perovskite film deposition, the device was finished by thermal evaporation of copper (100 nm) under vacuum. The device area is the overlap of the ITO substrate and copper electrode (area ~1 mm^2). The electrical measurement was done using Keithley 4200 source measure unit. The scanning rate for the *I-V* curve was 0.5 V s^{-1}. All samples were measured at room temperature and in air with humility lower than 30%. San-Electric XES-70S1 solar simulator provided the light source for light illumination (100 mW cm^{-2}), and a Si diode was used to calibrate the light intensity.

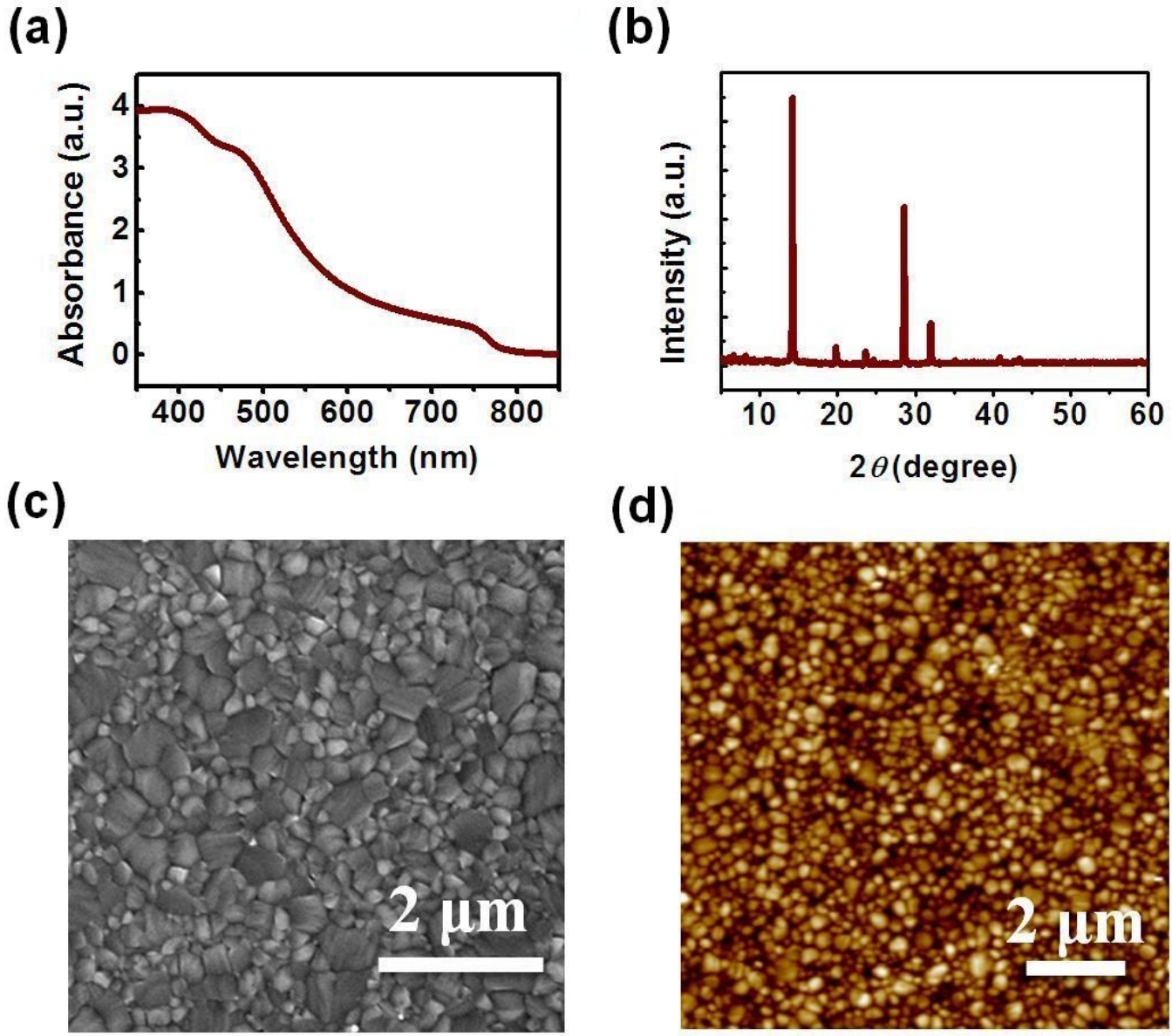

Fig. S1 Organic-Inorganic hybrid perovskite characterization. (a) UV-Vis absorbance of $CH_3NH_3PbI_3$ thin film on quartz. (b) X-Ray diffraction (XRD) spectrum of the perovskite material without Cu top electrode. (c) Scanning Electronic Microscope (SEM) image of the solution-processed perovskite film**.** (d) Atomic Force Microscope (AFM) image of the synthesized perovskite film**.**

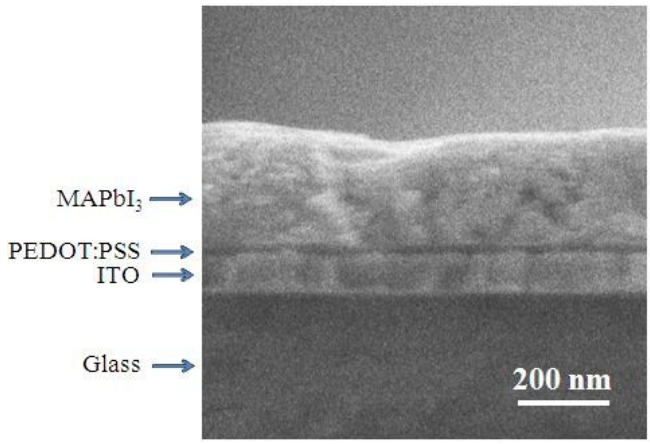

Fig. S2 Cross-sectional SEM image of sandwitched ITO/PEDOT:PSS/$CH_3NH_3PbI_3$ structure without top Cu electrode.

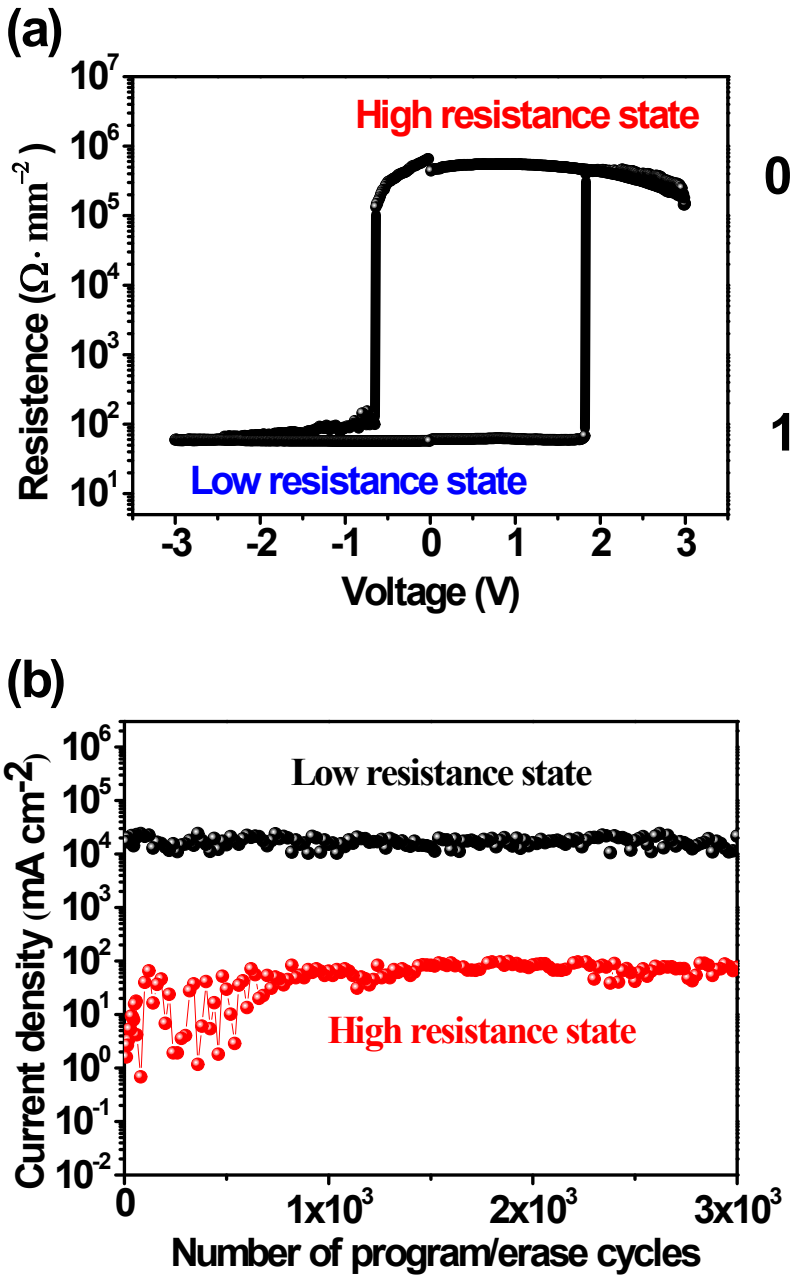

Fig. S3 Additional characterization of the memristive device. (a) Resistance-Voltage characteristics of the memristor device: ITO/PEDOT:PSS/$CH_3NH_3PbI_3$/Cu. (b) Endurance performance of ITO/PEDOT:PSS/$CH_3NH_3PbI_3$/Cu memristor device.

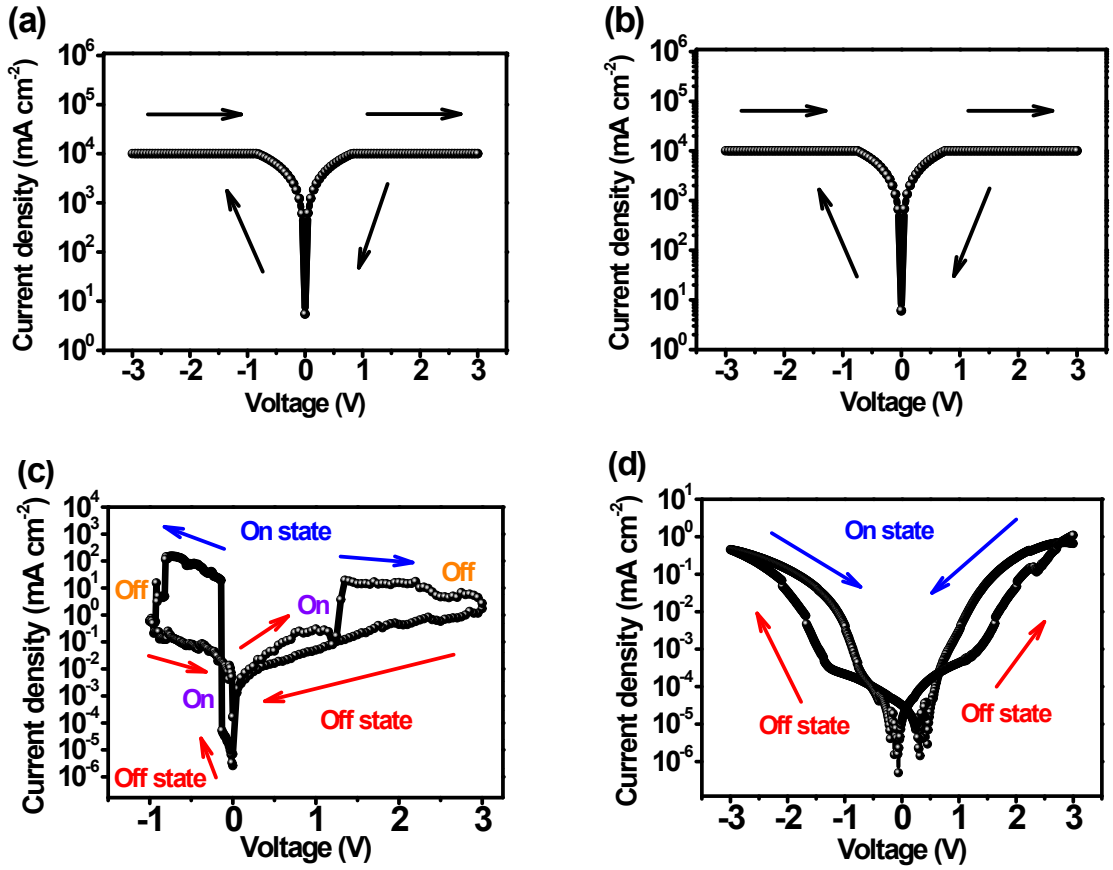

Fig. S4 Current-Voltage (*I-V*) characterization of the control devices. (a) Cu/$CH_3NH_3PbI_3$/Cu. (b) Cu/$CH_3NH_3PbI_3$/Au. (c) ITO/PEDOT:PSS/$CH_3NH_3PbI_3$/ITO. (d) ITO/PEDOT:PSS/$CH_3NH_3PbI_3$/Au

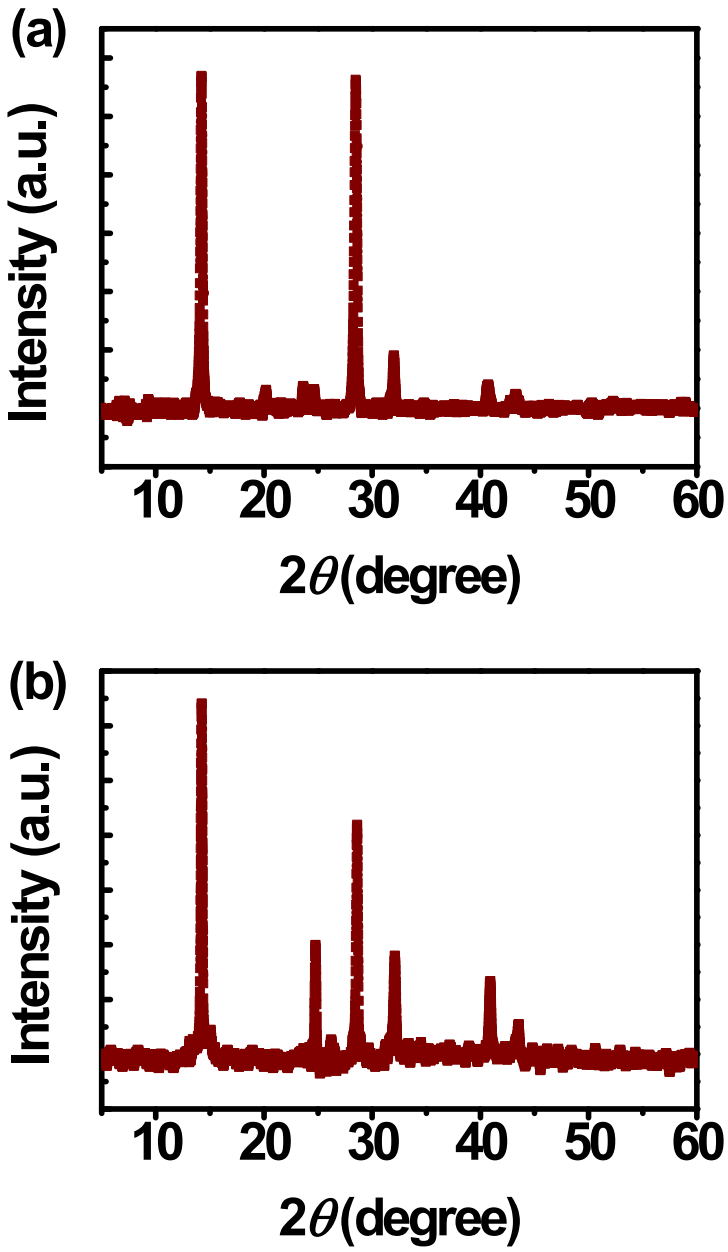

Fig. S5 X-Ray diffraction (XRD) spectra of (a) $CH_3NH_3PbI_{3-x}Cl_x$; (b) $CH_3NH_3Pb_{0.5}Sn_{0.5}I_3$.

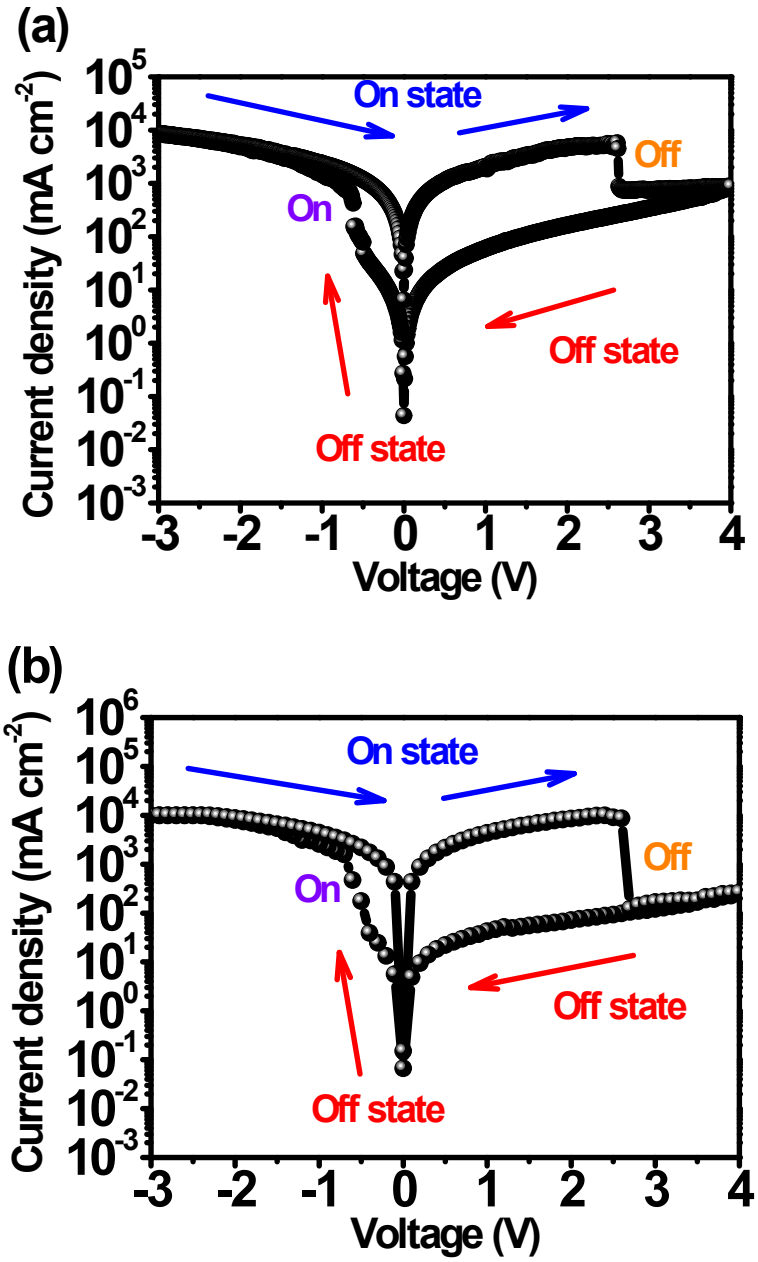

Fig. S6 *I-V* characteristics of the memristor devices with sandwich structure. (a) ITO/PEDOT:PSS/$CH_3NH_3PbI_{3-x}Cl_x$/Cu. (b) ITO/PEDOT:PSS/$CH_3NH_3Pb_{0.5}Sn_{0.5}I_3$/Cu.